# Neutron-scattering studies on CeM2Ge2 (M=Ag, Au, and Ru)

**Alois Loidl, K. Knorr, G. Knopp, Alexander Krimmel, R. Caspary, A. Böhm, G. Sparn, C. Geibel, Frank Steglich, A. P. Murani**

**Angaben zur Veröffentlichung / Publication details:**

Loidl, Alois, K. Knorr, G. Knopp, Alexander Krimmel, R. Caspary, A. Böhm, G. Sparn, C. Geibel, Frank Steglich, and A. P. Murani. 1992. "Neutron-scattering studies on CeM2Ge2 (M=Ag, Au, and Ru)." *Physical Review B* 46 (15): 9341–51. https://doi.org/10.1103/physrevb.46.9341.



# Neutron-scattering studies on $CeM_2Ge_2$ ($M$ = Ag, Au, and Ru)

A. Loidl
*Institut für Physik, Universität Mainz, W-6500 Mainz, Germany*
*and Institut für Festkörperphysik, Technische Hochschule Darmstadt, W-6100 Darmstadt, Germany*

K. Knorr and G. Knopp
*Institut für Physik, Universität Mainz, W-6500 Mainz, Germany*

A. Krimmel
*Institut für Physik, Universität Mainz, W-6500 Mainz, Germany*
*and Institut Laue Langevin, F-38042 Grenoble, France*

R. Caspary, A. Böhm, G. Sparn, C. Geibel, and F. Steglich
*Institut für Festkörperphysik, Technische Hochschule Darmstadt, W-6100 Darmstadt, Germany*

A. P. Murani
*Institut Laue Langevin, F-38042 Grenoble, France*
(Received 30 December 1991; revised manuscript received 23 June 1992)

The results of elastic, quasielastic, and inelastic neutron-scattering studies on polycrystalline $CeM_2Ge_2$ ($M$=Ag, Au, and Ru) are presented. All compounds reveal long-range magnetic order at low temperatures. Ferromagnetic ($M$=Ru), antiferromagnetic ($M$=Au), and incommensurate ($M$=Ag) structures were detected. Using time-of-flight (TOF) techniques, the crystalline electric-field splittings were determined. With high-resolution TOF experiments the temperature and wave-vector dependence of the magnetic relaxation rate was studied. Korringa-like behavior was found for the Au and Ru compounds. In $CeAg_2Ge_2$ the temperature dependence of the magnetic relaxation rate exhibits a square-root dependence at high temperatures and shows a residual linewidth for low $T$. This behavior can be explained by strong hybridization effects of the $f$ electrons with the delocalized band states which are active in heavy fermion systems. Previous results in $CeCu_2Ge_2$ and $CeNi_2Ge_2$ are included, whenever necessary. Detailed comparison is made with results obtained in the disilicides.

## I. INTRODUCTION

Kondo lattices, i.e., stoichiometric systems which contain Ce or U ions, have been studied intensively during the past decade. Depending on the strength of the hybridization of the $f$ electrons with delocalized band states, these compounds reveal very different ground-state properties: if the hybridization is small, crystal-field effects and Ruderman-Kittel-Kasuya-Yosida (RKKY) exchange interactions determine the low-temperature properties yielding magnetic order in most cases. In the limit of strong hybridization, charge fluctuations delocalize the $f$ electrons. Hence, the localized magnetic moments are lost and an enhanced Pauli paramagnetism characterizes these intermediate valence systems (IVS).[1] Heavy-fermion behavior shows up in a narrow range in between these limiting cases. Heavy-fermion systems (HFS) exhibit very unusual low-temperature properties:[2] an enormously enhanced linear term of the specific heat and, concomitantly, an enhanced, almost $T$-independent Pauli-spin susceptibility corresponding to high effective masses of the quasiparticles. The ground state of HFS can be quite different: a coherent heavy fermion state has been determined in, e.g., $CeCu_6$;[3] superconductivity (SC) has been reported for, e.g., $CeCu_2Si_4$ (Ref. 4) and $UBe_{13}$,[5] "heavy-fermion band magnetism" (HFBM) for, e.g., $CePb_3$ (Ref. 6) and $CeAl_3$.[7] Coexistence of SC and HFBM was found in $UPt_3$ (Ref. 8) and $URu_2Si_2$.[9] Here HFBM refers to a situation in which the magnetic degrees of freedom, originally connected with the localized $f$ electrons, have been promoted to the itinerant heavy quasiparticles.[10]

The tetragonal $CeM_2X_2$ homologs, where $M$ stands for some 3$d$ (Ni,Cu), 4$d$ (Ru,Ag), and 5$d$ (Au) transition metals and $X$ = Si or Ge, provide a rich variety of materials in which prototypical ground states of highly correlated electron systems can be investigated. Thermal neutron-scattering experiments which reveal both the elastic and inelastic magnetic neutron-scattering cross section have been performed mainly on the disilicide homologs: Long-range magnetic order for $M$ = Ag, Au, Pd, and Rh has been discovered by Grier *et al.*[11]

Magnetic relaxation rates, studied via an analysis of the paramagnetic quasielastic line, have been reported by Stassis *et al.*[12] and Uemura *et al.*[13] for $CeCu_2Si_2$. A systematic study of the spin dynamics of the disilicides $M$ = Au, Pd, Rh, and Ru was performed by Grier *et al.*[14] and Severing, Holland-Moritz, and Frick.[15] In single-

crystal work by Rossat-Mignod *et al.*[16] it has been possible to separate on-site (Kondo-like) and intersite (RKKY-like) interactions in $CeRu_2Si_2$. Crystal electric-field (CEF) excitations were studied for $M=$Cu by Horn *et al.*[17] and for $M=$Au, Ag, Pd, and Ru by Grier *et al.*[14] and Severing *et al.*[18] Much less is known for the digermanides: results of neutron-scattering studies in $CeCu_2Ge_2$ (Ref. 19) and $CeNi_2Ge_2$,[20] which have been obtained in the course of this work, were published previously. Preliminary results of CEF excitations and magnetic relaxation rates in $CeM_2Ge_2$ with $M=$Ag and Au are documented in Refs. 21–23.

Here we present detailed neutron-scattering studies on the elastic, quasielastic, and inelastic magnetic response in $CeM_2Ge_2$ for $M=$Ag, Au, and Ru. Whenever necessary, results obtained in $CeCu_2Ge$ (Ref. 19) and $CeNi_2Ge_2$ (Ref. 20) are included. Results of magnetic dc susceptibility, heat capacity, and thermal-expansion measurements in $CeAg_2Ge_2$, $CeAu_2Ge_2$, and $CeRu_2Ge_2$ have been reported by Böhm *et al.*,[24] Lang,[25] and Sparn.[26] These experiments revealed that the former two compounds order antiferromagnetically at $T_N=7$ K (Ag) and 16 K (Au). $CeRu_2Ge_2$ exhibits ferromagnetic order below $T_c=7.5$ K with weak indications for a second phase transition at 8.5 K. The silver and gold compounds show an enhanced term linear in $T$ of the specific heat well below the magnetic ordering temperatures. These anomalies have been interpreted[24] as the existence of heavy-mass electronic quasiparticles which coexist with the antiferromagnetic order.

## II. EXPERIMENTAL RESULTS AND ANALYSIS

Polycrystalline samples of $CeM_2Ge_2$ ($M=$Ag, Au, Ru) have been prepared from the elements by melting together appropriate amounts in an argon arc. X-ray diffraction showed that the compounds crystallize in the body-centered-tetragonal $ThCr_2Si_2$ structure. Thus they

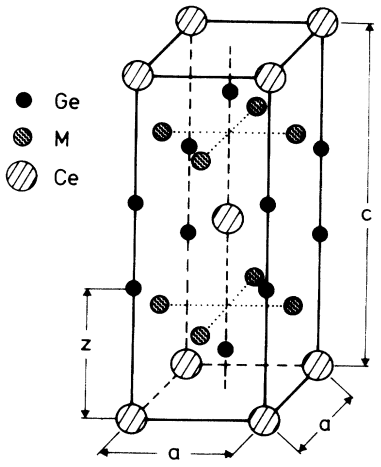


FIG. 1. Tetragonal unit cell of $CeM_2Ge_2$ ($ThCr_2Si_2$ structure).

are isomorphic to the prototype heavy-fermion system $CeCu_2Si_2$. The elementary cell is displayed in Fig. 1.

### A. Magnetic structures

The neutron-diffraction experiments have been carried out on the multidetector diffractometer D1B of the Institut Laue-Langevin using incident neutrons with a wavelength of 2.25 Å. Figure 2 shows the diffraction pattern of the Ag compound above (10 K) and below (1.5 K) the magnetic ordering temperature. The difference pattern $[I(1.5\text{ K})-I(10\text{ K})]$ is shown in the lowest frame of Fig. 2. For the Au and the Ru compounds, only the difference patterns are shown together with the difference patterns of both $CeAg_2Ge_2$ and $CeCu_2Ge_2$ (Ref. 19) in Fig. 3. The tetragonal lattice parameters $a$ and $c$ have been determined from the positions of the nuclear reflections. The $ThCr_2Si_2$ structure has one free position-

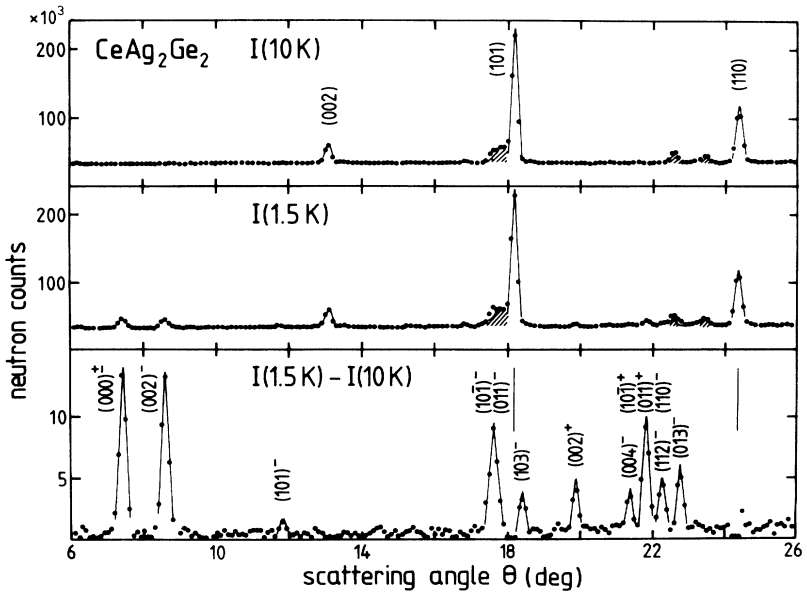


FIG. 2. Bragg scattering profiles for $CeAg_2Ge_2$: $T=10$ K (top) and $T=1.5$ K (middle). Shaded areas are nuclear reflections due to parasitic phases. Difference pattern $[I(1.5\text{ K})-I(10\text{ K})]$ yielding the magnetic Bragg reflections only (bottom).

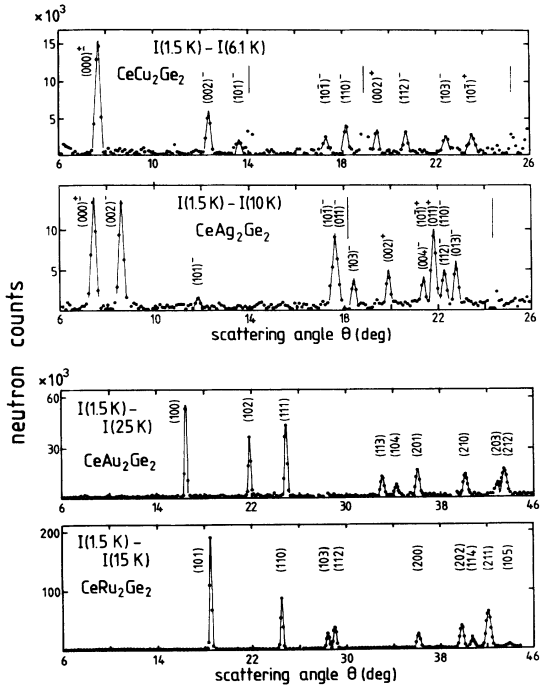


FIG. 3. Difference pattern for some digermanides with $M$=Cu, Ag, Au, and Ru: all Bragg reflections are of magnetic origin only.

al parameter, namely the $z$ coordinate of the Si atom. This parameter has been derived from a structure refinement based on the nuclear Bragg intensities. The structural parameters are compiled in Table I. The data on $CeCu_2Ge_2$ (Ref. 19) are included.

*$CeAg_2Ge_2$*. This compound shows a number of additional Bragg reflections at lowest temperatures, which are regarded as Bragg reflections of a magnetically ordered phase with a modulated arrangement of the magnetic moments. In such a structure the magnetic Bragg reflections appear at the positions $(hkl)^{\pm}=\tau_{hk}\pm\mathbf{q}_0$.

The components of $\mathbf{q}_0$ have been determined using a fit routine to the observed scattering angles in which the modulation vector $\mathbf{q}_0$ has been varied systematically within the irreducible part of the Brillouin zone. The positions of the magnetic reflections are well described with a modulation vector of $(0.285\pm0.015, 0\pm0.03, 0.90\pm0.01)$ in reduced units $2\pi/a$ and $2\pi/c$, respectively. The measured intensities have been compared to calculated values for different modulated structures. Two types of modulated spin arrangements have been examined: plane spirals and collinear arrangements where the length of the magnetic moment is modulated. Conical spirals can be excluded since there are no magnetic intensities at the position of the nuclear reflections. The best fit of the calculated magnetic intensities to the observed intensities is obtained with a static transverse spin wave with the spins along the $a$ axis and a magnetic moment of $(1.85\pm0.15)\mu_B$ at 1.5 K. The positions and the intensities of the magnetic reflections as observed and as calculated with this structural model are given in Table II. For the analysis three peaks have not been used: The $(101)^-$ reflection almost vanishes in the background noise of the difference pattern. The $(10\bar{1})^-$ reflection appears as a shoulder on the strong $(011)^-$ peak only. The $(103)^-$ reflection is at the position of the (101) nuclear reflection (see Fig. 2). The intensities of all the other reflections can well be reproduced. However, at low angles the intensities are systematically too small compared to the calculated values (Table II). Similar effects have been found in $CeAg_2Si_2$ by Grier *et al.*[11] and were interpreted in terms of deviations from the $Ce^{3+}$ form factor caused by polarization effects of the $4f$ electron by the band states. Within the accuracy of the diffraction measurement the modulation vector is temperature independent. The temperature dependence of the magnetic moment has been derived from the two strongest magnetic reflections (Fig. 4). The magnetic moment extrapolates to zero for temperatures between 6 and 6.5 K. Based on the specific-heat results a phase-transition temperature of 7 K has been suggested.[25]

*$CeAu_2Ge_2$*. The low-temperature diffraction pattern shows additional reflections at the positions $(hkl)$, $h+k+1=2n+1$, which are systematically absent in the chemical structure. Hence the magnetic structure is antiferromagnetic, with the two Ce ions of the tetragonal cell having antiparallel magnetic moments. The vanishing magnetic intensity at (001) indicates that the moments are aligned along the $c$ axis. The magnetic moment at 1.5

TABLE I. Lattice parameters $a$, $c$, and Si-coordinate $z$ in reduced coordinates at $T=1.5$ K; magnetic ordering temperatures: $T_N$ and $T_C$; ordered moment, as observed ($\mu_s$) and as calculated from the CEF ground state ($\mu_{calc}$); ordering wave vector $\mathbf{q}_0$ in units $2\pi/a$ and $2\pi/c$, spin directions s and spiral plane.

| $M$ | Cu | Ag | Au | Ru |
|---|---|---|---|---|
| $a$(Å) | 4.143(3) | 4.279(3) | 4.367(3) | 4.256(3) |
| $c$(Å) | 10.156(5) | 10.929(5) | 10.407(5) | 10.000(5) |
| $Z$ | 0.384(2) | 0.385(2) | 0.383(2) | 0.370(3) |
| $T_N, T_c$(K) | 4.15(2) | 6.3(2) | 16.0(5) | 8.7(2) |
| $\mu_s(\mu_B)$ | 0.77(5) | 1.50(10) | 1.88(5) | 1.98(3) |
| $\mu_{calc}(\mu_B)$ | 1.53 | 1.47 | 1.75 | 2.02 |
| $q_0$(r.l.u.) | (0.28,0.28,0.54) | (0.28,0,0.9) | (001) | (0,0,0) |
| $\mathbf{S}_{\parallel}$ | | a | c | c |
| spiral plane $\perp$ | $\mathbf{q}_0$ | | | |

TABLE II. Observed and calculated peak positions Θ and intensities $I$ in $CeAg_2Ge_2$, using a modulation vector $\mathbf{q}_0=(0.285,0,0.9)$ and assuming a transverse static spin wave with the spins directed along the $a$ axis. The fits have been performed excluding the $(101)^-$, $(101)^-$, and $(103)^-$ peaks. The intensities of these peaks have error bars ranging from 40–100 %. The $R$ factor corresponding to these results is 8.5%.

| $(hkl)\pm\mathbf{q}_0$ | $\Theta_{obs}$ | $\Theta_{calc}$ | $I_{obs}$ | $I_{calc}$ |
|---|---|---|---|---|
| $(000)^{\pm}$ | 7.62 | 7.67 | 3198(200) | 3952 |
| $(002)^-$ | 8.78 | 8.75 | 3150(200) | 3401 |
| $(101)^-$ | 12.00 | 12.14 | 180(180) | 9 |
| $(101)^-$ | 17.50 | 17.67 | 902(400) | 624 |
| $(011)^-$ | 17.82 | 17.79 | 2256(200) | 2148 |
| $(103)^-$ | 18.57 | 18.71 | 869(350) | 605 |
| $(002)^+$ | 20.07 | 20.19 | 974(80) | 855 |
| $(004)^-$ | 21.57 | 21.57 | 816(80) | 743 |
| $(011)^+$ | | | | |
| $(110)^-$ | 22.02 | 22.10 | 2370(150) | 2452 |
| $(101)^+$ | | | | |
| $(112)^-$ | 22.47 | 22.49 | 1080(100) | 1008 |
| $(013)^-$ | 22.97 | 22.95 | 1263(100) | 1307 |

K is $(1.88\pm0.05)\mu_B$. The temperature dependence of the ordered moment is shown in Fig. 4. The temperature dependence suggests a magnetic ordering temperature of about 16 K, in good agreement with susceptibility and thermal-expansion measurements.[24]

*$CeRu_2Ge_2$.* At low temperatures the diffraction pattern exhibits extra intensity only on nuclear reflections.

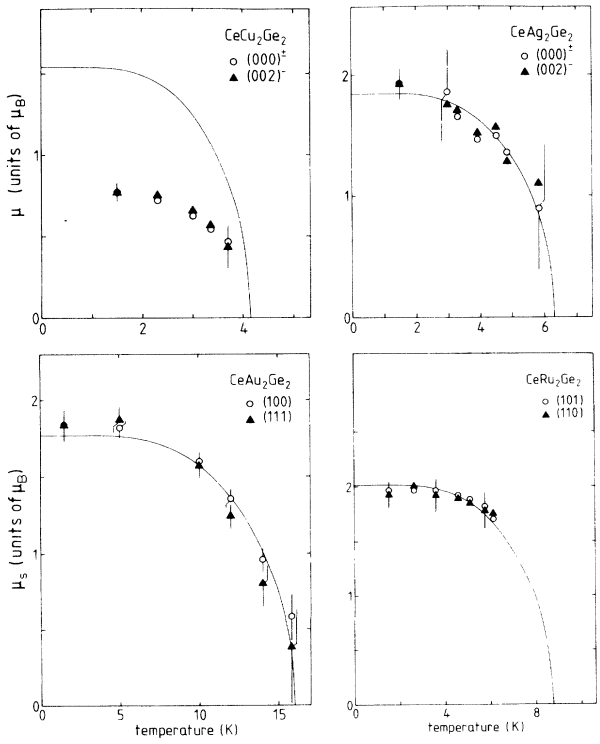


FIG. 4. Temperature dependence of the ordered magnetic moment determined from the peak intensities as indicated. The solid line is a mean-field calculation of $\mu_s$ utilizing the appropriate ground state of the $Ce^{3+}$ ion in the crystal electric field; see Refs. 21–23.

Hence the magnetic structure is ferromagnetic. The absence of an extra contribution to the (002) reflection requires that the ordered moments point along the $c$ axis. Its value at 1.5 K is $(1.98\pm0.03)\mu_B$. Its temperature dependence has been followed only up to 6.3 K (Fig. 4). The heat capacity data suggest two transitions, a strong ferromagnetic transition at 7.5 K and weak indications of a second transition at 8.5 K.

*$CeCu_2Ge_2$.* We recall that this compound orders antiferromagnetically in a plane spiral arrangement at 4.15 K. The moment is $0.74\mu_B$ at 1.5 K (see Fig. 4), the ordering wave vector $\mathbf{q}_0=(0.28,0.28,0.54)$. The rotation plane of the moments is perpendicular to $\mathbf{q}_0$ (Ref. 18; see also Table II).

### B. Crystal-field excitations

Inelastic neutron-scattering experiments have been carried out on the time-of-flight spectrometer IN4 of the Institute Laue-Langevin. Incident neutron energies of 12.5, 30, and 50 meV were utilized. Arrays of detectors have been centered at scattering angles between 18° and 100°. Each sample has been studied at least at three temperatures, typically $T\gtrsim T_N$, 100 K, and 200 K. The time-of-flight spectra have been converted into energy spectra $S(\omega)$ after correcting them for background scattering and absorption losses as determined from reference measurements on the empty sample holder and on Cd and V standards. Magnetic excitations are discriminated from phonon excitations through their dependences on both momentum transfer and temperature. In addition, the measurements on the Ce compounds have been complemented by measurements on the corresponding (nonmagnetic) La compounds. No attempt was made, however, to convert the La spectra into fictitious phonon spectra of the Ce compound.

In the $ThCr_2Si_2$ structure the two Ce sites are equivalent and of tetragonal symmetry. The crystal-field operator is a linear combination of the operators $O_2^0, O_4^0$, and $O_4^4$ with the coefficients $B_2^0, B_4^0$, and $B_4^4$. The $J=\frac{5}{2}$

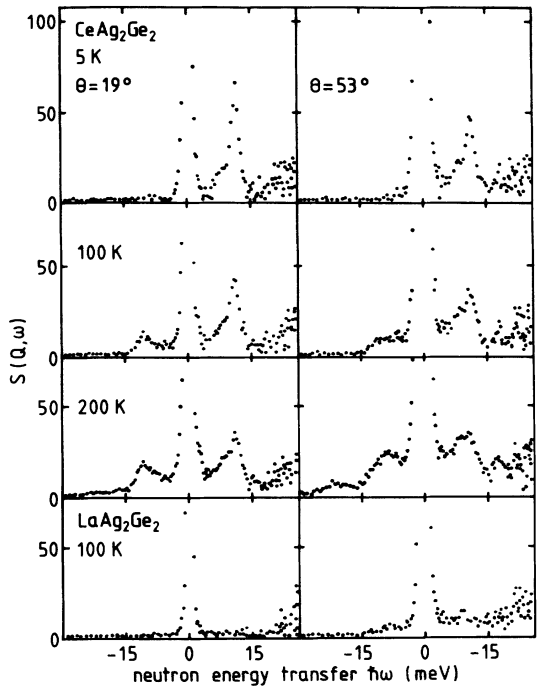


FIG. 5. Scattering law as a function of neutron energy transfer for two different average scattering angles (left row: $\Theta=19°$; right row: $\Theta=53°$) for $CeAg_2Ge_2$ at 5, 100, and 200 K and for $LaAg_2Ge_2$ at 100 K.

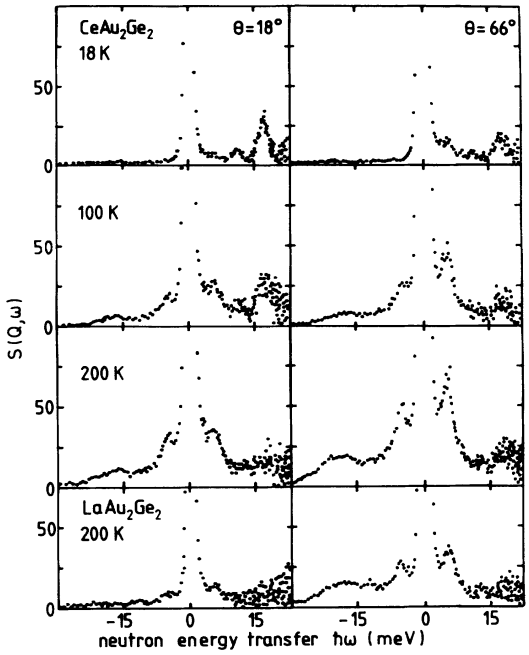


FIG. 6. Scattering law as a function of neutron energy transfer for two different average scattering angles (left row: $\Theta=18°$; right row: $\Theta=66°$) for $CeAu_2Ge_2$ at 18, 100, and 200, and for $LaAu_2Ge_2$ at 200 K.

ground multiplet of the $Ce^{3+}$ ion is split into three doublets. The almost trivalent state of the Ce ion in the present compounds is well established, e.g., by the susceptibility measurements.[24] Since in the general case, the three doublets are connected pairwise by magnetic dipole transitions, one expects to observe three crystal-field excitations in the neutron-scattering spectra.

*$CeAg_2Ge_2$.* This compound shows only one crystal-field transition at 11 meV, which is clearly visible both in excitation and deexcitation (Fig. 5). Assuming that there are no further crystal-field transitions with energies outside the range of energy transfers accessible with the spectrometer (in the case of $CeAg_2Ge_2$ the accessible energy range was $\lesssim 40$ meV), one ends up with an effective double-quartet level scheme. Taking into account the value of the ordered moment (cf. Table I), two sets of crystal-field parameters can be suggested depending on whether the ground state is a doublet or a quartet. Specific-heat experiments[24] favor a quartet ground state, and so does the fact that in this case the easy direction is along **a**; whereas in the other case the easy direction is along **c**, which would be difficult to reconcile with the spins pointing along **a**.

*$CeAu_2Ge$.* The spectra are shown in Fig. 6. At 18 K two excitations at energy transfers of 11 and 17 meV are observed in down scattering, which are thus attributed to the transitions from the crystal-field ground state to the excited states. A smaller signal is detected at about 7 meV. Its intensity increases in contrast to the crystal-field transitions with scattering angle (i.e., with momentum transfer) and with temperature. It is also clearly seen in the spectrum of the La compound. Hence it is attributed to phonons. The spectra recorded at 100 and 200 K yield no additional information on the crystal-field excitations. In particular it is difficult to decide whether

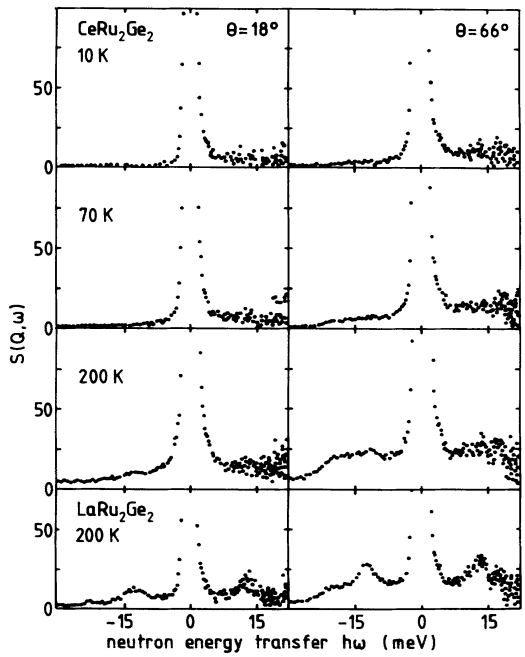


FIG. 7. Scattering law as a function of neutron energy transfer for two different average scattering angles (left row: $\Theta=18°$; right row: $\Theta=66°$) for $CeRu_2Ge_2$ at 10, 70, and 200 K and for $LaRu_2Ge_2$ at 200 K.

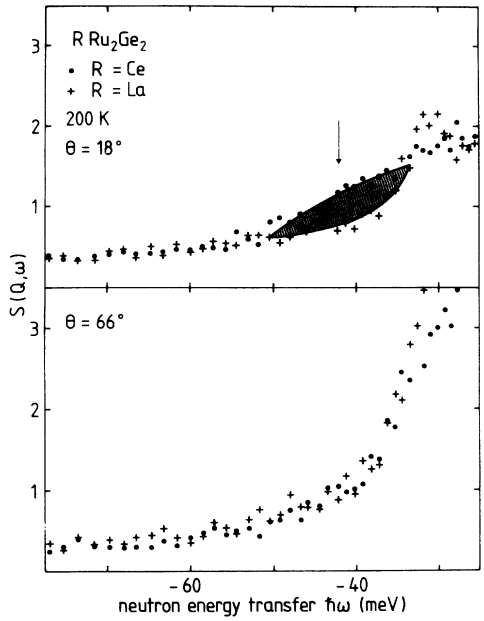


FIG. 8. Scattering law versus neutron energy gain in $CeRu_2Ge_2$(·) and $LaRu_2Ge_2$ (+) at 200 K. Top: Average scattering angle $\Theta=18°$. The shaded area indicates some inelastic-scattering intensity in addition to the quasielastic one for the Ru compound, possibly due to a CEF excitations at 40 meV. Bottom: Average scattering angle $\Theta=66°$.

a transition between the two excited crystal-field states is actually present, since its excitation energy would coincide with the energy of the phonon state. The two excitation energies and the intensity ratio of the excitations as observed at 18 K are sufficient to determine the crystal-field parameters. The ground state is almost pure $J_z=\pm\frac{5}{2}$ with a small admixture of $\pm\frac{3}{2}$.

*$CeRu_2Ge_2$.* Clear indications for crystal-field transitions for $\hbar\omega<20$ meV have not been observed (Fig. 7). The specific-heat experiments suggest excited crystal-field states at about 43 and 65 meV.[27] These energies are too high to be seen on the neutron energy-loss side of the spectra where the accessible range of energy transfers extends from 0 to about $\frac{2}{3}$ of the incident energy. Comparing the 200-K spectra at scattering angles of 18° and 66° one observes in fact an excess intensity on the neutron energy-gain side of the 18° spectrum at energy transfer of

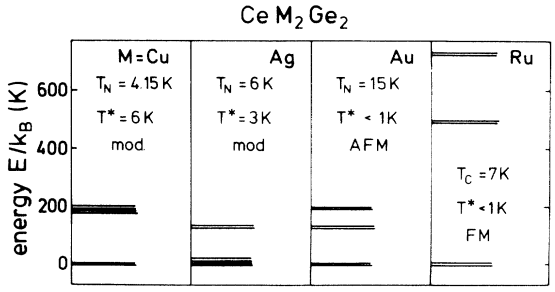


FIG. 9. Energies of the crystal electric field levels in $CeM_2Ge_2$ compounds ($M$ = Cu, Ag, Au, and Ru). Characteristic temperatures and types of the magnetic order are indicated.

approximately 42 meV (Fig. 8). This deexcitation energy compares nicely to the lower doublet as determined in the specific-heat experiment.[27] Figure 8 reveals no indications of a second transition at 65 meV. However, in this energy range the scattered neutron intensities are too low to yield reliable results and we trust the level scheme from Ref. 27.

The level scheme of the CEF split ground multiplet, the CEF parameters, the calculated moment, and the easy axis are indicated in Table III. A survey of the CEF splitting in the digermaindes is given in Fig. 9.

*$CeCu_2Ge_2$.* The crystal-field levels have been determined previously. The pertinent information is included in Fig. 9 and Table III.

### C. Magnetic relaxation rates

The low-energy part of the magnetic excitation spectrum has been studied on the time-of-flight spectrometer IN6 of the Institut Laue-Langevin, using incident neutrons of 3.15 meV. Again the time-of-flight spectra have been converted into energy spectra. The quasielastic contributions can be approximately described by Lorentzian distributions, properly decorated by the thermal population factor. Superimposed on the quasielastic magnetic contribution is the incoherent scattering, which is well described by a Gaussian profile, the width of which is given by the energy resolution of the spectrometer (0.09 meV at $\omega=0$). The Lorentzian width $\Gamma$ [half width at half maximum (HWHM)] is regarded as the magnetic (spin) relaxation rate, introduced by interactions of the $f$

TABLE III. CEF level scheme and parameters for $CeM_2Ge_2$: first and second excited level $E_1$ and $E_2$, CEF parameters $B_m^n$ and coefficients of the eignestates $a$ and $b$. Error bars are indicated only for the CEF parameters in the Au compound. Here a fit to the neutron intensities has been performed. For the other compounds the CEF parameters were determined using information of different experimental techniques. These parameters should be read as the most reliable ones, consistent with all results (see also Ref. 19). Ground state ($E_0=0$): $a|\pm\frac{5}{2}\rangle-b|\mp\frac{3}{2}\rangle$. First excited state ($E_1$): $|\pm|\frac{1}{2}\rangle$. Second excited state ($E_2$): $b|\pm\frac{5}{2}\rangle+a|\mp\frac{3}{2}\rangle$.

| $M$ | $E_1$ | $E_2$ | $B_2^0$ | $B_4^0$ | $B_4^4$ | $a$ | $b$ | $\mu_{calc}$ | Easy axis |
|---|---|---|---|---|---|---|---|---|---|
| | (K) | | | (K) | | | | ($\mu_B$) | |
| Au | 127(10) | 197(15) | −6.4(9) | −0.27(6) | 2.6(4) | 0.926 | 0.379 | 1.75(10) | $c$ |
| Ag | 0 | 128(10) | 6.5 | 0.097 | 1.23 | 0.285 | −0.959 | 1.85 | $a$ |
| Cu | 191(10) | 191(10) | −8.78 | −0.055 | 2.79 | 0.900 | 0.436 | 1.53 | $c$ |
| Ru | 500(30) | 750 | −30.50 | −1.311 | 5.41 | 0.980 | 0.200 | 2.02 | $c$ |

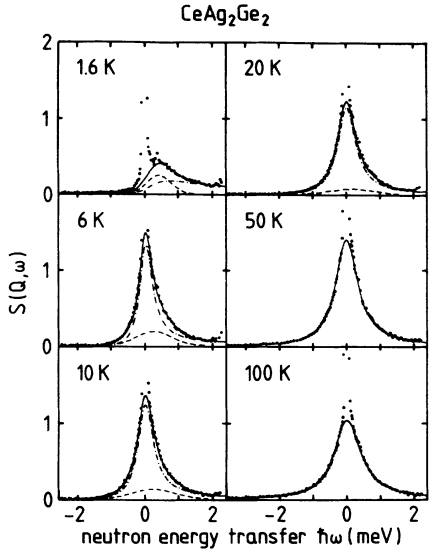


FIG. 10. Scattering law versus neutron energy transfer for $CeAg_2Ge_2$ at different temperatures. The solid lines represent the results of fits using a superposition of Lorentzian (dashed-dotted lines) and Gaussian contributions (dashed lines).

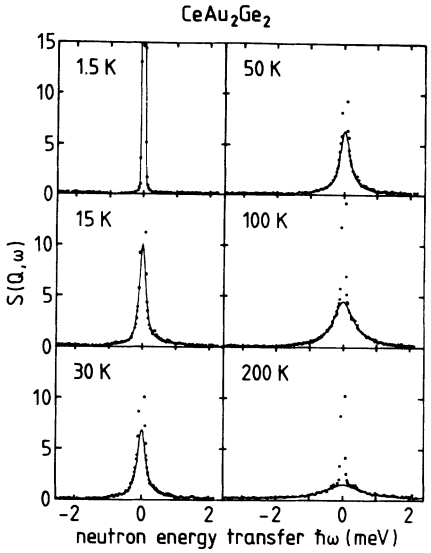


FIG. 11. Scattering law versus neutron energy transfer in $CeAu_2Ge_2$ at different temperatures. The solid lines are the results of fits using a Lorentzian line shape. At the lowest temperature ($T < T_N$) the quasielastic component is absent. The resolution-limited Gaussian peak is due to elastic incoherent scattering processes and has not been fitted at higher temperatures.

electrons with the band states. In rare-earth compounds with a stable $4f$ configuration one expects Korringa-type behavior for the quasielastic line with $\Gamma \propto T$. Due to strong hybridization effects the magnetic relaxation rates in heavy-fermion compounds behave completely differently: theoretical calculations of the dynamic susceptibility revealed that for $T \ll T_K$ the quasielastic line should show distinct deviations from a Lorentzian line shape[28] and that $\Gamma(T)$ deviates significantly from a linear $T$ dependence. Theoretically it has been predicted[29] that $\Gamma(T)$ approaches a residual finite value for $T \to 0$ and exhibits a square-root dependence at high temperatures ($T \gg T_K$).

*$CeAg_2Ge_2$.* Above 30 K the quasielastic spectrum can well be described by a Lorentzian line shape (Fig. 10). For $T \leq 30$ K the quality of the fits is considerably improved by using quasielastic profiles composed of a Lorentzian and an additional Gaussian component. Also for $T \geq T_N = 6$ K the Gaussian profile is centered at zero energy transfer. In the magnetically ordered phase the quasielastic Lorentzian persists, down to the lowest temperatures. The Gaussian contribution is shifted to a finite energy transfer of 0.2 meV at 1.5 K.

*$CeAu_2Ge_2$.* The spectra $S(Q,\omega)$ vs neutron energy transfer $\hbar\omega$ are shown in Fig. 11 for different temperatures. Above the magnetic ordering temperature ($T_N = 16$ K) a quasielastic component is present and can be well described by a Lorentzian profile. In the antiferromagnetic phase the spectrum reveals a resolution-limited Gaussian peak only. The quasielastic component is absent as expected for a classical magnetic system where the magnetic response is concentrated in the magnetic Bragg reflections and magnon-type excitations.

*$CeRu_2Ge_2$.* $S(Q,\omega,T)$ vs $\hbar\omega$ (Fig. 12) behaves analogously to the former compound: Lorentzian profiles were found in the paramagnetic state. In the ferromagnetic phase ($T_c = 7$ K) no quasielastic contributions can be detected in the frequency range investigated.

Fits to the neutron-scattering profiles, shown as solid lines in Figs. 10–12, yield the temperature dependence of the widths and of the intensities of the Lorentzian (and Gaussian) contributions. In the Au and Ru compounds (Figs. 11 and 12) the quasielastic coherent intensities can

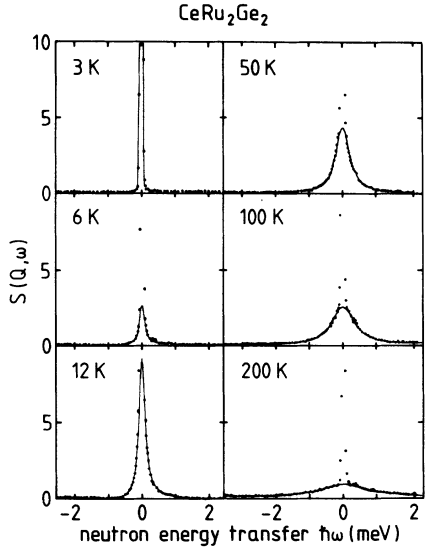


FIG. 12. Scattering law versus neutron energy transfer in $CeRu_2Ge_2$ at different temperatures. The solid lines are the results of fits using a Lorentzian line shape. At the lowest temperature ($T < T_N$) the quasielastic component is absent. The resolution limited Gaussian peak is due to elastic incoherent scattering processes and has not been fitted at higher temperatures.

be well described by Lorentzian line shapes at all temperatures. The width $\Gamma$ (half width and half maximum) narrows considerably with decreasing $T$. At the lowest temperatures in the magnetically ordered states, only the elastic incoherent scattering contributions can be detected which are described by a narrow Gaussian profile the width of which corresponds to the energy resolution of the spectrometer at zero energy transfer. Fits to the elastic incoherent contributions are shown at low $T$ only, but, for clarity, are omitted at higher temperatures.

For $CeAg_2Ge_2$ the profiles are composed of a superposition of Gaussian (width: $\Gamma_G$; intensity: $A_G$) and Lorentzian (width: $\Gamma_L$; intensity: $A_L$) components. The results of the fits are shown in Fig. 10 where the solid lines correspond to the best fits using composed profiles. The dashed lines represent the Gaussian, the dashed-dotted line the Lorentzian contribution. At $T \gtrsim 30$ K the intensities of the Gaussian component $A_G$ are negligibly small.

The residual linewidth ($\Gamma_L$ for $M$ = Ag, $\Gamma$ for $M$ = Au and Ru) gives an estimate of the characteristic energy scale $k_B T^*$ of the Kondo lattice ($T^*$ corresponds to the usual Kondo temperature $T_K$ in the single-ion case). $\Gamma(T)$ for $CeAu_2Ge_2$ and $CeRu_2Ge_2$ is shown in Fig. 13. For both compounds the magnetic relaxation rate reveals a linear (Korringa-type) temperature dependence. The residual linewidth at the lowest temperatures coincides with the width of the experimental resolution. Thus we give an estimate of $T^* < 1$ K for these two compounds. The results for $CeAg_2Ge_2$ are shown in Fig. 14. The temperature dependence of the Lorentzian width $\Gamma_L$ reveals significant deviations from a linear Korringa-type behavior and exhibits a residual linewidth of approximately 0.25 meV at $T_N$, yielding a characteristic temperature $T^* \simeq 3$ K. Below $T_N$, $\Gamma_L$ increases strongly toward low temperatures. A similar behavior has been observed in $U_2Zn_{17}$ by Broholm *et al.*[30] These authors stated that $\hbar\Gamma$ is inversely proportional to the density $n(\epsilon_F)$ of quasiparticle states at the Fermi energy and thus, that the increase of $\Gamma$ signals the decrease of $n(\epsilon_F)$. In $CeAg_2Ge_2$ a finite density of quasiparticle states for $T < T_N$ is in accordance with specific-heat results[24] which demonstrate

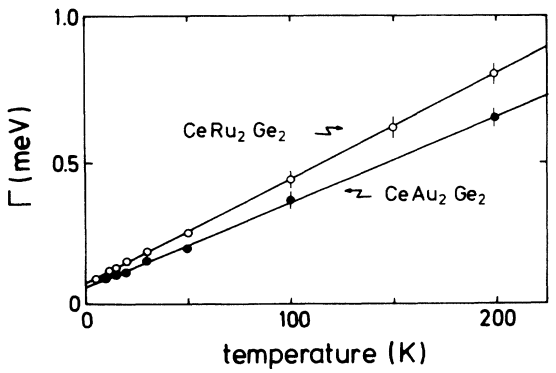


FIG. 13. Temperature dependence of the quasielastic linewidth (HWHM) for $CeRu_2Ge_2$ and $CeAu_2Ge_2$. The residual linewidth coincides with the experimental resolution of the spectrometer.

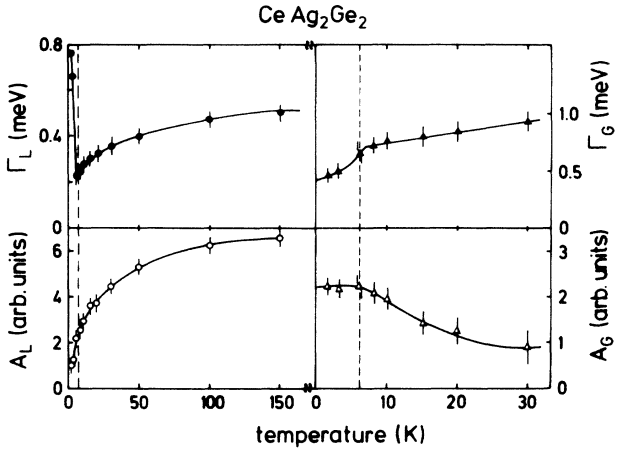


FIG. 14. Temperature dependence of the widths (HWHM) $\Gamma$ (upper row; full symbols) and intensities $A$ (lower row; open symbols) of the Lorentzian (left row; circles) and Gaussian components (right row; triangles) in $CeAg_2Ge_2$.

that renormalized electronic quasiparticles coexist with antiferromagnetic order. The quasielastic scattering intensity $A_L/T$ closely follows $\chi(T)$, where $\chi(T)$ is the static magnetic susceptibility.[31] Following Ref. 32 we interpret the Gaussian component as being associated with critical spin fluctuations, which develop due to intersite RKKY interactions. As demonstrated in Fig. 14, with decreasing temperatures the lifetime of these states ($\sim 1/\Gamma_G$) increase, while their weight $A_G$ increases toward $T_N$ and remains constant for $T < T_N$. In the magnetically ordered state they correspond to magnon states with an average excitation energy of 0.2 meV.

## III. DISCUSSION AND CONCLUSIONS

As our neutron-diffraction results show, $CeRu_2Ge_2$ reveals ferromagnetic and $CeAu_2Ge_2$ antiferromagnetic order, whereas the compounds with $M$ = Ag and Cu exhibit spiral structures implying a propagation vector incommensurate with the nuclear lattice. In the corresponding disilicides only the compounds with $M$ = Ag and Au show magnetic order at low temperatures: In the Au disilicide antiferromagnetism is established; the Ag disilicide reveals a modulated structure.[11] According to Fig. 4 sizable effects of moment compensation due to hybridization effects can be resolved for $CeCu_2Ge_2$ only. Indeed only for this compound $T^*$ and the Néel temperature $T_N$ are of comparable size (Table IV).

Modulated structures which are incommensurate with the nuclear lattice, including spirals and static spin waves, are rather common in $RM_2X_2$ compounds ($R$ = rare earth) with $ThCr_2Si_2$ structure.[33] The modulation wave vector $\mathbf{q}_0$ in all these compounds is of the order of the wave vector of the Fermi surface and thus determined by RKKY interactions between local magnetic moments. This kind of magnetic ordering is labeled "local-moment magnetism" (LMM) in the following. Guided by theoretical predictions,[10] a transition from LMM to HFBM, where the magnetic degrees of freedom

TABLE IV. Magnetic ordering temperatures $T_m$ (a: antiferromagnetic; f: ferromagnetic) (Refs. 19 and 24–26), characteristic temperatures $T^*$ ($T^*$ corresponds to the Kondo temperature $T_K$ in the single-ion case) and fit parameters of the parametrization of the temperature dependence of the relaxation rates $\Gamma_0$ and $\gamma$ in $CeM_2Ge_2$

| $M$ | $T_m$ | $T^*$ | $\Gamma_0$ | $\gamma$ |
|---|---|---|---|---|
| | [K] | [K] | [K] | ($K^{1/2}$) |
| Cu | 4.15[a] | 6±1.5 | 1.4±0.1 | 1.34±0.04 |
| Ag | 6.3[a] | 3±1 | 2.0±0.15 | 0.35±0.02 |
| Au | 16.0[a] | <1 | | |
| Ru | 8.7[f] | <1 | | |
| Ni | | 30 (Ref. 20) | 0 | 5.3±0.1 |

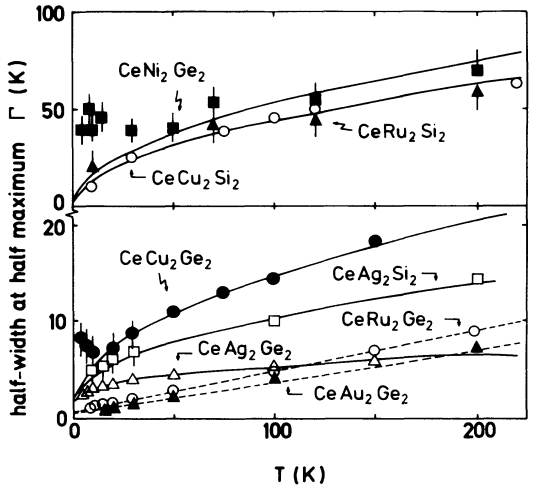


FIG. 15. Temperature dependence of the quasielastic Lorentzian linewidth in $CeM_2X_2$ compounds; upper frame: $CeNi_2Ge_2$ (■) and $CeRu_2Si_2$ (▲); for comparison: $CeCu_2Si_2$ (○) (Ref. 12). Lower frame: $CeCu_2Ge_2$ (●); $CeAg_2Si_2$ (□); $CeAg_2Ge_2$ (△); $CeAu_2Ge_2$ (▲), and $CeRu_2Ge_2$ (○). The solid lines represent fits using a square-root dependence of $\Gamma(T)$. The dashed lines indicate the linear Korringa-type behavior of $CeAu_2Ge_2$ and $CeRu_2Ge_2$.

have been transferred to the itinerant heavy quasiparticles, has recently been experimentally verified in $Ce(Cu_{1-x}Ni_x)_2Ge_2$.[34]

A summary of the CEF level schemes for the digermanides investigated in the course of this work has been given in Fig. 9 and Table III. From the site symmetry of the Ce ion, three doublets are expected in all cases. However, for both Cu and Ag an accidental degeneracy yields a quartet, it being the excited state in the Cu digermanide but the ground state in the Ag compound. Gunnarson and Schönhammer[35] calculated the dynamic susceptibility for Kondo systems including crystal-field effects and spin-orbit splittings. They showed that the crystal-field excitation is not located at $E_{CF}$ but instead at $\hbar\omega = E_{CEF} + k_B T^*$. In the systems under consideration this effect appears to be unimportant as we always find $E_{CEF} \gg k_B T^*$. However, it is worthwhile to mention that the linewidths of the CEF transitions seem to scale with the hybridization strength.[21]

Finally we performed a study of the temperature and wave-vector dependence of the magnetic relaxation rates in the digermanides, including a detailed line-shape analysis. The latter yielded Lorentzian line shapes in the two limiting extremes of Kondo and LMM systems, respectively: (i) in the Kondo limit, the line shape can be described by pure Lorentzian behavior, e.g., in $CeNi_2Ge_2$;[20] (ii) local-moment magnets with $T_N \gg T^*$, e.g., $CeAu_2Ge_2$, again show pure Lorentzian line shapes of the quasielastic scattered intensities for $T \gtrsim T_N$. Heavy-fermion systems with $T_N \approx T^*$ exhibit a more complex behavior: in order to obtain satisfactory fits, the line shapes in $CeAg_2Ge_2$ and $CeCu_2Ge_2$ had to be analyzed including Lorentzian and Gaussian components in the quasielastic scattering. We propose that these different components originate from a competition of on-site and intersite correlations. Single-crystal work is needed to verify this proposal in more detail.

The temperature dependences of the Lorentzian widths are summarized in Fig. 15. Here we included the results of $CeNi_2Ge_2$ (Ref. 20), $CeCu_2Si_2$ (Ref. 17), and $CeCu_2Ge_2$ (Ref. 19) which have been published earlier and some unpublished results for $CeAg_2Si_2$ and $CeRu_2Si_2$ (Ref. 36). These two disilicides have been investigated in detail by Severing *et al.*[15,18] Only the ferromagnet $CeRu_2Ge_2$ and the antiferromagnetic $CeAg_2Ge_2$ reveal Korringa-like behavior.

The high-temperature behavior of the line shapes of all the other compounds can be approximately described by a square-root dependence.[37] We parametrized the temperature dependence of the linewidth $\Gamma$ (HWHM) assuming $\Gamma(T) = \Gamma_0 + \gamma\sqrt{T}$ (solid lines in Fig. 15). The fit parameters $\Gamma_0$ and $\gamma$ for $M$=Cu, Ag, and Ni are listed in Table IV. Theoretically, universal behavior was predicted for $\Gamma(T)$:[29] a constant linewidth ($\Gamma \approx T^*$) for $T < T^*$ and a square-root dependence for $T \gg T^*$. In the digermanides this behavior can be found in $CeNi_2Ge_2$ (Fig. 15), for all the other compounds the low-temperature residual linewidth is masked by the onset of the magnetic order. Here we took the linewidth $\Gamma(T \approx T_N)$ as the measure of the characteristic temperature $T^*$.

A closer inspection of Table IV shows that $T^*$ and $\gamma$ are strongly correlated while $\Gamma_0$ seems to be of minor relevance only. From the universal behavior of the high-temperature square-root dependence[29] it follows that $\gamma = \text{const} \cdot \sqrt{T^*}$, with the constant depending on the degeneracy of the ground state.

The Fermi-liquid description of the heavy-fermion state makes some specific predictions for the imaginary part of the magnetic susceptibility. For example, a linear dependence of the magnetic relaxation rates on the momentum transfer $Q$ is expected within the framework of Fermi-liquid theory. In all the digermanides investigated $\Gamma$ is almost independent of $Q$ over a wide range of momentum transfers (0.4 $\text{Å}^{-1} \lesssim Q \lesssim 2.3$ $\text{Å}^{-1}$). However, we have to admit that only $CeNi_2Ge_2$ was investigated for temperatures $T \ll T^*$, i.e., in the Fermi-liquid state.

Finally, Fig. 16 demonstrates the dominating role of the hybridization between the $4f$ states and the ligand

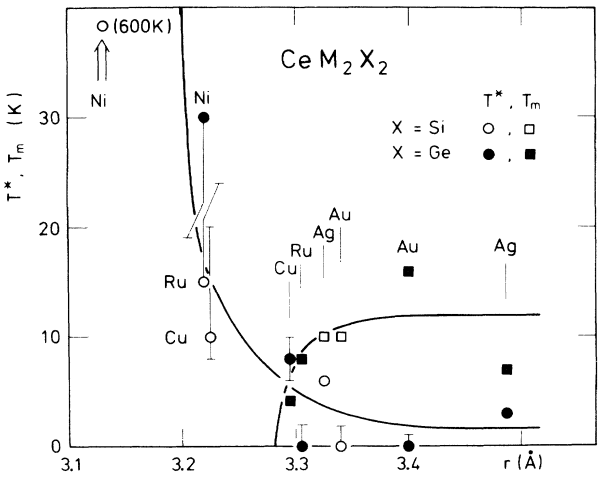


FIG. 16. Kondo-lattice temperature $T^*$, from low-$T$ quasielastic neutron linewidths (circles) as well as entropy, thermal expansion and thermopower (bars), and magnetic ordering temperatures $T_m$ in $CeM_2Si_2$ and $CeM_2Ge_2$ versus $r$, the Cerium-transition metal ($M$) distance ($M$ =Cu, Ag, Au, Ni, Ru). Lines are drawn to guide the eye.

($M$)-derived $d$ states: Here we plotted the characteristic temperatures, namely the Kondo-lattice temperature $T^*$ and the magnetic ordering temperatures $T_m$, versus the separation $r$ between Ce and the ligand $M$ in the series $CeM_2X_2$ with $M$ =Cu, Ag, Au, Ni, Ru, and $X$ =Si (Refs. 11 and 15) and Ge (Refs. 24, 36, and 38). It is assumed that $r$ correlates inversely with the hybridization strength, which can be expressed by the local exchange coupling constant $g = n(\epsilon_F)\cdot J$, where $n(\epsilon_F)$ is the density of states at the Fermi level and $J<0$ the exchange integral. In the extreme case of very weak ($|g| \ll 1$) and very strong ($|g|>1$) hybridization, magnetic ordering between stable local $f$ moments and an intermediate-valence state are observed, respectively. Heavy fermions develop in a narrow range (3.2 Å $< r <$ 3.3 Å) where the energies for the on-site moment compensation $T^*$ and for the intersite indirect exchange interaction $T_{RKKY}$ are of the same order. Because of the different dependences on $g$[$T_{RKKY} \propto g^2$, $T^* \propto \exp(1/g)$] one expects[39] a sharp drop in $T_m$ upon increasing $f$-$d$ hybridization. In Fig. 16 this is clearly observed near $r$ = 3.3 Å.

## ACKNOWLEDGMENTS

This work was supported by the Bundesministerium für Forschung und Technologie under Contract No. 03-LO1MAI and by the Sonderforschungsbereich 252, Darmstadt/Frankfurt/Mainz/Stuttgart. We thank H. Spille for his help in the susceptibility experiments and for useful discussions.

[1]For reviews, see D. Wohlleben, J. Phys. C **4**, 231 (1976); J. M. Lawrence, P. S. Riseborough, and R. D. Parks, Rep. Prog. Phys. **44**, 1 (1981).

[2]For reviews, see G. R. Stewart, Rev. Mod. Phys. **56**, 755 (1984); C. M. Varma, Comments Solid State Phys. **11**, 221 (1985); H. R. Ott, Prog. Low Temp. Phys. **11**, 215 (1987); P. Fulde, J. Keller, and G. Zwicknagl, Solid State Phys. **41**, 1 1988; N. Grewe and F. Steglich, *Handbook on the Physics and Chemistry of Rare Earths,* edited by K. A. Gschneidner, Jr. and L. L. Eyring (Elsevier, Amsterdam, 1991), Vol 14, p. 343.

[3]Y. Onuki, Y. Shimizu, and T. Komatsubara, J. Phys. Soc. Jpn. **53**, 1210 (1984); G. R. Stewart, Z. Fisk, and M. S. Wire, Phys. Rev. B **30**, 482 (1984).

[4]F. Steglich, J. Aarts, C. D. Bredl, W. Lieke, D. Meschede, W. Franz, and H. Schäfer, Phys. Rev. Lett. **43**, 1982 (1979).

[5]H. R. Ott, H. Rudigier, Z. Fisk, and J. L. Smith, Phys. Rev. Lett. **50**, 1595 (1983).

[6]C. L. Lin, J. Teter, J. E. Crow, T. Mihalisin, J. Brooks, A. I. Abou-Aly, and G. R. Stewart, Phys. Rev. Lett. **54**, 2541 (1985); C. Vettier, P. Morin, and J. Floquet, *ibid.* **56**, 1980 (1986).

[7]S. Barth, H. R. Ott, F. N. Gygax, B. Hitti, E. Lippelt, and A. Schenck, J. Magn. Magn. Mater. **76&77**, 455 (1988); D. Jaccard, H. Sierro, J. P. Brison, and J. Flouquet, J. Phys. (Paris) Colloq. **49**, C8-741 (1988).

[8]G. Aeppli, E. Bucher, C. Broholm, J. K. Kjems, J. Baumann, and J. Hufnagel, Phys. Rev. Lett. **60**, 615 (1988).

[9]C. Broholm, J. K. Kjems, W. J. L. Buyers, P. Matthews, T. T. M. Palstra, A. A. Menovskya, and J. A. Mydosh, Phys. Rev. Lett. **58**, 1467 (1987).

[10]N. Grewe and B. Welslau, Solid State Commun. **65**, 437 (1988); B. Welslau and N. Grewe, Physica B **165&166**, 387 (1990); See also N. Grewe and F. Steglich (Ref. 2).

[11]B. H. Grier, J. M. Lawerence, V. Murgai, and R. D. Parks, Phys. Rev. B **29**, 2664 (1984).

[12]C. Stassis, B. Batlogg, J. P. Remeika, J. D. Axe, G. Shirane, and Y. J. Uemura, Phys. Rev. B **33**, 1680 (1986).

[13]Y. J. Uemura, C. F. Majkrzak, G. Shirane, C. Stassis, G. Aeppli, B. Batlogg, and J. P. Remeika, Phys. Rev. B **33**, 6508 (1986).

[14]B. H. Grier, J. M. Lawrence, S. Horn, and J. D. Thompson, J Phys. C **21**, 1099 (1988).

[15]A. Severing, E. Holland-Moritz, and B. Frick, Phys. Rev. B **39**, 4164 (1989).

[16]J. Rossat-Mignod, L. P. Regnault, J. L. Jacoud, C. Vettier, P. Lejay, J. Flouquet, E. Walker, D. Jaccard, and A. Amato, J. Magn. Magn. Mater. **76&77**, 376 (1988).

[17]S. Horn, E. Holland-Moritz, M. Loewenhaupt, F. Steglich, H. Scheuer, A. Benoit, and J. Flouquet, Phys. Rev. B **23**, 3171 (1981).

[18]A. Severing, E. Holland-Moritz, B. D. Rainford, S. R. Culverhouse, and B. Frick, Phys. Rev. B **39**, 2557 (1989).

[19]G. Knopp, A. Loidl, K. Knorr, L. Pawlak, M. Duczmal, R. Caspary, U. Gottwick, H. Spille, F. Steglich, and A. P. Murani, Z. Phys. B **77**, 95 (1989).

[20]G. Knopp, A. Loidl, R. Caspary, U. Gottwick, C. D. Bredl, H. Spille, F. Steglich, and A. P. Murani, J. Magn. Magn. Mater. **74**, 341 (1988).

[21]G. Knopp, H. Spille, A. Loidl, K. Knorr, U. Rauchschwalbe, R. Felten, G. Weber, F. Steglich, and A. P. Murani, J. Magn. Magn. Mater. **63&64**, 88 (1987).
[22]G. Knopp, A. Loidl, K. Knorr, H. Spille, F. Steglich, and A. P. Murani, J. Magn. Magn. Mater. **76&77**, 420 (1988).
[23]A. Loidl, G. Knopp, H. Spille, F. Steglich, and A. P. Murani, Physica B **156&157**, 794 (1989).
[24]A. Böhm, R. Caspary, U. Habel, L. Pawlak, A. Zuber, F. Steglich, and A. Loidl, J. Magn. Magn. Mater. **76&77**, 150 (1988).
[25]M. Lang, Ph.D. thesis, TH Darmstadt, 1990 (unpublished).
[26]G. Sparn, Ph.D. thesis, TH Darmstadt, 1990 (unpublished).
[27]H. Rietschel, B. Renker, R. Felten, F. Steglich, and G. Weber, J. Magn. Magn. Mater. **76&77**, 105 (1988).
[28]A. Auerbach, Fu H. Kim, K. Levin, and M. R. Norman, Phys. Rev. Lett. **60**, 623 (1988).
[29]N. E. Bickers, D. L. Cox, and J. W. Wilkins, Phys. Rev. Lett. **54**, 239 (1985).
[30]C. Broholm, J. K. Kjems, G. Aeppli, Z. Fisk, J. L. Smith, S. M. Shapiro, G. Shirane, and H. R. Ott, Phys. Rev. Lett. **58**, 917 (1987).
[31]A. Böhm, diploma thesis, TH Darmstadt, 1988 (unpublished).
[32]U. Walter, M. Loewenhaupt, E. Holland-Moritz, and W. Schlabitz, Phys. Rev. B **36**, 1981 (1987).
[33]J. Leciejewicz and A. Szytula, J. Magn. Magn. Mater. **63&64**, 190 (1987).
[34]F. Steglich, G. Sparn, R. Moog, S. Horn, A. Grauel, M. Lang, M. Nowak, A. Loidl, A. Krimmel, K. Knorr, A. P. Murani, and M. Tachiki, Physica B **163**, 19 (1990); F. Steglich, C. Geibel, S. Horn, U. Ahlheim, M. Lang, G. Sparn, A. Loidl, A. Krimmel, and W. Assmus, J. Magn. Magn. Mater. **90&91**, 383 (1990).
[35]O. Gunnarson, and K. Schönhammer, J. Magn. Magn. Mater. **52**, 227 (1985).
[36]G. Knopp, Ph.D. thesis, University Mainz, 1989 (unpublished).
[37]S. Horn, F. Steglich, E. Holland-Moritz, and M. Loewenhaupt, Physica **107B**, 103 (1981).
[38]R. Moog, diploma thesis, TH Darmstadt, 1990 (unpublished); M. Nowak, diploma thesis, TH Darmstadt, 1989 (unpublished); A. Grauel, diploma thesis, TH Darmstadt, 1989 (unpublished).
[39]S. Doniach, Physica **91B**, 231 (1977).